The Cryosphere Discuss., 8, 1279–1304, 2014
www.the-cryosphere-discuss.net/8/1279/2014/
doi:10.5194/tcd-8-1279-2014

The Cryosphere
Discussions
Open Access

How much snow falls on the Antarctic ice sheet?

C. Palerme[1,2], J. E. Kay[3], C. Genthon[1,2], T. L'Ecuyer[4], N. B. Wood[5], and C. Claud[6]

[1]CNRS, LGGE (UMR5183), 38041 Grenoble, France
[2]Univ. Grenoble Alpes, LGGE (UMR5183), 38041 Grenoble, France
[3]NCAR CGD – National Center for Atmospheric Research Climate and Global Dynamics, Boulder, Colorado, USA
[4]Department of Atmospheric and Oceanic Sciences, University of Wisconsin-Madison, USA
[5]Cooperative Institute for Meteorological Satellite Studies, University of Wisconsin-Madison, USA
[6]Laboratoire de Météorologie Dynamique/IPSL, CNRS, Ecole Polytechnique, Palaiseau, France

Received: 7 February 2014 – Accepted: 13 February 2014 – Published: 24 February 2014

Correspondence to: C. Palerme (cyril.palerme@lgge.obs.ujf-grenoble.fr)

Published by Copernicus Publications on behalf of the European Geosciences Union.

Abstract

Climate models predict Antarctic precipitation to increase during the 21st century, but their present day Antarctic precipitation differs. A fully model-independent climatology of the Antarctic precipitation characteristics, such as snowfall rates and frequency, is needed to assess the models, but was not available so far. Satellite observation of precipitation by active spaceborne sensors has been possible in the polar regions since the launch of CloudSat in 2006. Here we use CloudSat products to build the first multi-year model-independent climatology of Antarctic precipitation. The mean snowfall rate from August 2006 to April 2011 is 171 mm yr^{-1} over the Antarctic ice sheet north of 82° S. The ECMWF ERA Interim dataset agrees well with the new satellite climatology.

1 Introduction

Evaluating Antarctic accumulation, the sum of precipitation, evaporation, melt, run-off, and blowing snow (Eisen et al., 2008), is a major challenge with relevance to sea level rise. While no significant change in Antarctic accumulation has been found in ice cores and reanalysis products over the last 50 yr (Monaghan et al., 2006; Frezzotti et al., 2013), future changes are likely which will have global consequences: over the 21st century, a 25 % increase in accumulation would result in a drop of approximately 1.6 mm yr^{-1} in global sea level (Gregory and Huybrechts, 2006). Because precipitation is an integral part of Antarctic accumulation, this study focuses on the challenging problem of documenting Antarctic precipitation from observation to benchmark climate models.

Climate models consistently predict Antarctic precipitation to increase in a warming climate (Church et al., 2013), but their present day mean Antarctic precipitation differs widely: from 150 to 550 mm yr^{-1} in the CMIP3 archive (Genthon et al., 2009a). There is therefore a need to understand the processes controlling Antarctic precipitation rates, and to evaluate climate models with precipitation observations.

While accumulation rates have been assessed using satellite and in situ measurements (Arthern et al., 2006; Eisen et al., 2008), precipitation characteristics such as the frequency and the rate remain poorly known. Ground-based measurements are sparse and difficult to make in Antarctica. In coastal areas, katabatic winds are strong, which makes the distinction between blowing snow and precipitation difficult. On the Antarctic plateau, the annual accumulation is small (few centimeters per year, Bromwich et al., 2004), and the instrumentation must be able to detect very light precipitation. In addition, low temperatures and hoarfrost negatively impact instruments that are not designed for harsh environments.

Precipitation characteristics depend greatly on the region in Antarctica. In coastal areas, precipitation is influenced by synoptic scale features such as cyclones and fronts (Bromwich, 1988). In the interior ($> 2500\,\text{m}$), a considerable part of the precipitation falls in the form of “diamond dust” (ice crystals) under clear sky conditions (Fujita and Abe, 2006).

In the past, passive microwave remote sensing has been used to detect new snow accumulation, using changes in surface emissivity (Bindschadler et al., 2005). However the method did not give quantities, and was found to be affected by other processes such as temperature and surface roughness.

Observations from the Cloud Profiling Radar (CPR) on CloudSat provide the first opportunity to measure precipitation in polar regions from a spaceborne radar (Stephens et al., 2008; Liu, 2008). With data available from August 2006 to April 2011, CloudSat directly observes snow precipitating through the atmosphere, rather than after it has been accumulated on the surface.

While several algorithms have been tested for precipitation over polar regions using CloudSat (Kulie and Bennartz, 2009; Hiley et al., 2010), no precipitation climatology have been done over Antarctica. In this study, we used two CloudSat products to make the first multi-year climatology of Antarctic precipitation from spaceborne observations.

2 Data and methods

The CPR, onboard CloudSat, is a nadir-looking radar at 94 GHz which measures the power backscattered by hydrometeors according to the distance from the sensor. It provides radar reflectivity profiles divided into 150 bins at a vertical resolution of 240 m, with a 1.7 km × 1.3 km footprint, and up to 82° of latitude. Its minimum detectable radar reflectivity is around −28 dBZ.

In this study, two CloudSat products are used to determine characteristics of Antarctic precipitation. The first product, 2C-PRECIP-COLUMN (Haynes et al., 2009), is used to assess the phase and occurence frequency of Antarctic precipitation. 2C-PRECIP-COLUMN provides a precipitation flag based on the near-surface reflectivity (dBZ) at the fourth bin over the ocean (between 600 and 840 m above the surface), and at the sixth bin over land (about 1300 m) to remove surface contamination (ground clutter). The phase is obtained by the temperature at 2 m predicted by the European Centre for Medium Range Weather Forecasts (ECMWF) weather analysis, and a model of melting layer with a constant lapse rate of $6\,^{\circ}\mathrm{C\,km^{-1}}$. According to the phase, different thresholds are applied to the near surface reflectivity to determine a likelihood of precipitation (possible or certain). Thus, the precipitation flags inform about the likelihood and the phase of precipitation.

The second product, 2C-SNOW-PROFILE (Wood, 2011; Wood et al., 2013) is used to assess the snowfall rates. 2C-SNOW-PROFILE retrieves estimates of liquid-equivalent snowfall rate for profiles where 2C-PRECIP-COLUMN indicates “snow possible” or “snow certain”, or where 2C-PRECIP-COLUMN indicates “mixed possible” or “mixed certain” and the estimated melted mass fraction at the surface is less than or equal to 0.1. Using a priori estimates of snow particle size distribution, microphysical and scattering properties, an optimal estimation retrieval (Rodgers, 2000) is performed for the contiguous layer of snow-containing radar bins nearest the surface, with exclusions for likely ground clutter contamination. With this approach, the so-called Z-S relationship between radar reflectivity and snowfall rate is not fixed, but can vary subject to the constraints of the reflectivity profile and the a priori expectations.

The retrieval also provides estimated uncertainties for the retrieved snowfall rates. The uncertainties depend on the uncertainties in the observed reflectivities as well as those in the simulated reflectivities provided by the retrieval's radar forward model. These uncertainties arise due to measurement error and due to the approximate nature of the forward model and its a priori assumptions. To the extent they can be characterized, systematic errors are removed. Within the context of the retrieval algorithm the remaining uncertainties are considered to be unbiased and random; however, these likely consist of some combination of systematic and random uncertainties since, for example, the algorithm's a priori assumptions are not tuned to the particular characteristics of Antarctic snowfall. Thus, while climatological averaging of retrieved snowfall rates reduces the truly random component of the uncertainties, some indeterminate bias is likely also present, and its evaluation is an ongoing area of research.

In this study, both CloudSat datasets are processed over a grid of 1° of latitude by 2° of longitude between 63° S and 82° S. The number of orbits per grid cell for the period August 2006–April 2011 is shown in Fig. 1. Over the Antarctic continent, the number of orbits per grid cell is at least 350 for the entire period, which represents one orbit every 5 days.

CloudSat products provide the data along their orbit. In order to map the 2C-PRECIP-COLUMN data over a grid of 1° by 2°, one flag per grid cell overflown is retained for each orbit. First, for the precipitation frequency, flags are sorted into three classes: no precipitation, precipitation possible, and precipitation certain. Then, if all the flags in the same grid cell indicate no precipitation, no precipitation is retained. If at least one flag indicates precipitation certain in the grid cell, precipitation certain is retained. And if there is no flag indicating precipitation certain, and at least one flag indicating precipitation possible, precipitation possible is retained.

To map the precipitation phase, flags are sorted into four classes: no precipitation, liquid, mixed, and solid precipitation. If the flags in the grid cell indicate no precipitation and precipitation, but only one precipitation phase, this phase is retained. If the flags in the same grid cell indicate rain and mixed precipitation, mixed precipitation and snow, or rain and snow, mixed precipitation is retained.

For the snowfall rate and its uncertainty from the 2C-SNOW-PROFILE product, the mean value in the grid cell has been retained for each orbit.

CloudSat observations have been compared to ERA Interim reanalysis in this study. ERA Interim is the latest global atmospheric reanalysis, which was produced by the European Centre for Medium Range Weather Forecasts (ECMWF) (Simmons et al., 2006). ERA Interim provides reanalysis from 1979 to present at a 6 hourly resolution. Its coverage is global at a spatial resolution of about 0.75° × 0.75°. The 6 h forecasts of precipitation are used here. Data from surface observations and radiosondes, commercial aircraft observations, and satellites measurements are assimilated in the numerical model to improve and constrain the forecasts (Dee et al., 2011). No precipitation observation is inserted in the numerical model, but precipitation is predicted by the model using other observations such as temperature and humidity.

3 Results

3.1 Precipitation characteristics from CloudSat

Figure 2 shows two maps of the precipitation frequency assessed from the 2C-PRECIP-COLUMN flags, and the difference between the two maps. The first map represents the proportion of flags indicating precipitation certain, and the second map, the proportion of flags indicating precipitation certain and possible.

The mean precipitation frequency (% of time) observed by CloudSat on the Antarctic continent (latitude < 82° S) is 14 % when the flags precipitation possible are not taken into account, and 26 % with the flags precipitation possible included. The spatial pattern of the precipitation frequency shows two distinct regions. The first area includes the West Antarctic ice sheet (WAIS) and the peripheral part of the East Antarctic ice sheet (EAIS), which corresponds approximately to the part of the continent with surface elevation below 2250 m. In this region, relatively high precipitation frequency is observed by CloudSat (between 22 % and 34 % depending if the flags precipitation possible are taken into account). The second region is the Antarctic plateau in East Antarctica (with surface elevation > 2250 m), and where the precipitation frequency observed by CloudSat is much lower (between 5 % and 19 %). Figure 3 shows the parts of the ice sheet with surface elevation over and below 2250 m derived from combined satellite radar and laser data (Bamber et al., 2009). Each part represents 50 % of the surface of the Antarctic ice sheet.

Precipitation phase has also been studied from the 2C-PRECIP-COLUMN flags. Only flags indicating precipitation certain were taken into account. Over the Antarctic ice sheet (latitude $< 82°$ S), solid precipitation represents 99.60 %, mixed precipitation 0.32 %, and rain 0.08 % of the precipitation occurrence (similar results have been found with the flags indicating precipitation possible included). In peripheral areas (surface elevation < 2250 m), mixed precipitation represents 0.63 % and rain 0.15 % of the precipitation occurrence. A lot of liquid and mixed precipitation occur over the Peninsula compared to the rest of the ice sheet (mixed precipitation contributes for 4.10 %, and rain for 1.32 % of the precipitation occurrence over this region). Furthermore, on the Antarctic plateau (surface elevation > 2250 m), all the precipitation is solid.

Because snowfall rate in the 2C-SNOW-PROFILE product is only estimated when the melted fraction is assessed to be less than or equal to 0.1, this product is well-suited to examining precipitation over Antarctica. Figure 4 shows the mean annual snowfall rate, the snowfall rate uncertainty, and the ratio of the uncertainty over the snowfall rate from the 2C-SNOW-PROFILE data. The mean snowfall rate observed by CloudSat on the Antarctic continent (latitude $< 82°$ S) is 171 mm water equivalent (w.e.) per year. However, the spatial pattern of the snowfall rate shows considerable differences between West Antarctica and East Antarctica. In West Antarctica, the mean annual snowfall rate is 303 mm w.e. yr^{-1}, compared to 118 mm w.e. yr^{-1} in East Antarctica. Furthermore, the mean snowfall rate over the peripheral part of the ice sheet (with surface elevation < 2250 m) is 303 mm w.e. yr^{-1}, compared to 36 mm w.e. yr^{-1} for the interior of the ice sheet (with surface elevation > 2250 m).

The map of the snowfall rate uncertainty in Fig. 4 represents the mean value of the single retrieval uncertainty for all the snowfall rate retrievals from August 2006 to April 2011. These are the expected uncertainties for individual snowfall rate retrievals and as noted earlier likely consist of both random and systematic components. Considering the maps in Fig. 4, 2C-SNOW-PROFILE product provides a snowfall rate uncertainty between 1.5 and 2.5 times the snowfall rate. This uncertainty is particularly high on the Antarctic plateau and the Peninsula, and it is lower on the peripheral part of the ice sheet and in West Antarctica. When calculating mean values with large number of observations, the standard error of the mean decreases as the number of samples increases. Therefore, in this study, the uncertainty on a 4.7 yr mean snowfall rate should be fairly small. However, the real snowfall rate uncertainty on the entire CloudSat period is difficult to assess because the part of systematic and random errors remain unknown.

3.2 Comparison of the CloudSat products to ERA Interim reanalysis

Table 1 shows a comparison between ERA Interim reanalysis and the precipitation flags from CloudSat at the French station Dumont d'Urville (Fig. 3). The ability of ERA Interim to represent precipitation in Antarctica is poorly known, but it is expected that observations assimilated in the model help to constrain the forecasts. It is important to note that CloudSat observations are not used to produce ERA Interim reanalysis (Dee et al., 2011). Field observations and radiosoundings are performed in Dumont d'Urville and assimilated in ERA Interim. Particularly, humidity profiles obtained by radiosounding are used to predict precipitation in ERA Interim. Therefore, precipitation predicted by ERA Interim should be relatively reliable in Dumont d'Urville.

Comparisons of the ERA Interim reanalysis data at Dumont D'Urville station against the precipitation flags from CloudSat were used to establish a precipitation rate threshold for comparing the datasets. A threshold of 0.07 mm/6 h for the ERA Interim precipitation rates was found empirically to give good agreement with the CloudSat precipitation flags. From 2006 to 2011, 67 % of the time, the ERA Interim precipitation rates at Dumont D'Urville were below this rate. During this period, for the 265 flags that indicate no precipitation, 92 % match with no precipitation in ERA Interim. Furthermore, for the 38 flags indicating precipitation possible, 55 % match with a precipitation event in ERA Interim. And for the 85 flags indicating precipitation certain, the success rate was 91 %.

A similar comparison on three latitude transects is shown in Fig. 5. The threshold used in ERA Interim was the same than in Dumont d'Urville (0.07 mm 6 h^{-1}). The value of the appropriate threshold seems to depend of the location in Antarctica, and it is likely lower where the precipitation rate is small. Overall, the success rate for the flags "precipitation certain" and "precipitation possible" is better near the coast than in the interior of the ice sheet. It could be due to the threshold applied to ERA Interim precipitation which could be too high for the Antarctic interior. Moreover shallow precipitation missed by CloudSat, and CloudSat sensitivity to very light snowfalls that occur in the interior could induce this difference.

Figure 5 shows also a curve of the Heidke skill score. The Heidke skill score measures the accuracy of forecasts relative to random forecasts (Barnston, 1992). It can vary between −1 and 1. A Heidke skill score equal to 0 means that forecasts are only due to chance, and it is equal to 1 for perfect forecasts. If the Heidke skill score is positive, the forecasts are better than random forecasts. Here, flags sorted as precipitation certain and period without precipitation are used. Figure 5 shows better agreement between CloudSat and ERA Interim (higher Heidke skill score) over peripheral areas than over the interior.

Even if precipitation is not assimilated in ERA Interim, observations assimilated as humidity profiles are more numerous in peripheral areas than in the Antarctic interior. Therefore, ERA Interim should be more reliable in peripheral areas than on the Antarctic plateau. This could help explain why there is better agreement between CloudSat and ERA Interim in peripheral areas than in the interior of the ice sheet.

A comparison between the snowfall rate observed by CloudSat and simulated by ERA Interim is shown in Fig. 6 and in Table 2. Over the Antarctic continent (latitude < 82 ° S), the mean snowfall rate is 171 mm w.e. yr^{-1} for CloudSat and 163 mm w.e. yr^{-1} for ERA Interim. The ratio of the snowfall rate observed by CloudSat and predicted by ERA Interim is relatively homogeneous over the ice sheet, except over parts of the Peninsula, the Vinson massif, and the Prince Charles Mountains, where it is very high. Orographic precipitation could be seen by CloudSat, but not predicted by ERA Interim due to the difference in spatial resolution between both datasets. However, ground clutter should be stronger over mountainous areas than over flat terrain, and may induce a spuriously high snowfall rate.

3.3 Comparison of the CloudSat products to the accumulation rate assessed by Arthern et al. (2006)

Table 2 and Fig. 7 show a comparison between the snowfall rate obtained by CloudSat for the period August 2006–April 2011, and the accumuation rate assessed by Arthern et al. (2006) for the period 1950–2000. Arthern et al. (2006) used in-situ glaciological measurements to assess the accumulation, and passive radiometer data (AMSR-E) sensitive to snowpack characteristics for interpolating their results.

Assuming that accumulation has not significantly changed during the last 50 yr (Monaghan et al., 2006; Frezzotti et al., 2013), the snowfall rate observed by CloudSat is higher than the accumulation over the periphery of the ice sheet, which is expected due to the negative contribution to accumulation of evaporation, melt, run-off, and blowing snow.

However, the snowfall rate observed by CloudSat is lower than the accumulation in the interior. Snowfall rate assessed by CloudSat over the interior of the ice sheet may be underestimated due to shallow precipitation missed by CloudSat and the weak reflectivity of small hydrometeors. Additionally, Genthon et al. (2009b) have shown that ground-based measurements used to produce the accumulation map from Arthern et al. (2006) were not filtered according to their accuracy, which would lead to an overestimated accumulation in the interior of the ice sheet.

Furthermore, modelling studies have suggested that deposition (inverse sublimation) could be stronger than evaporation at some locations in the interior of the ice sheet (Genthon and Krinner, 2001). Thus, hoarfrost formation could contribute significantly to the accumulation, and precipitation could be lower than accumulation in these regions.

4 Discussion and conclusion

A climatology of the Antarctic precipitation, the single most important positive term of the ice sheet mass balance, was still lacking so far. Filling this gap, Antarctic precipitation features such as the frequency, the phase, and the snowfall rate have been determined here using CloudSat products. CloudSat is the first spaceborne radar able to observe precipitation in Antarctica, and its potential has been demonstrated in this survey. The mean snowfall rate from August 2006 to April 2011 is 171 $\mathrm{mm\,yr^{-1}}$ over the Antarctic ice sheet north of 82° S, and the accumulation represents 95 % of the snowfall over this region.

However, due to assumptions about particle size distribution, particle masses, shapes and fallspeeds, snowfall rate assessed in the 2C-SNOW-PROFILE product has large uncertainties. In the 2C-PRECIP-COLUMN dataset, a large number of flags are sorted as "precipitation possible". This leads to a considerable range of precipitation frequency, even if the frequency estimated is probably more reliable than the snowfall rate. Moreover, on the Antarctic plateau, 2C-PRECIP-COLUMN algorithm may have difficulties in distinguishing precipitating from non precipitating hydrometeors due to their small particle size. The reflectivity thresholds applied in this algorithm could be too high for this kind of precipitation. Figure 8 shows a map of the ratio of the number of flags indicating precipitation possible over the number of flags indicating precipitation possible and certain. On the Antarctic plateau, most of the flags indicating precipitation are sorted as possible. Near surface reflectivity is sensitive to the size of hydrometeors, and on the plateau, particles are probably too small to increase the near surface reflectivity above the threshold "precipitation certain".

CloudSat is likely more accurate in peripheral areas than in the interior. Shallow precipitation (< 1300 m), missed by CloudSat, could be an important contribution to precipitation on the Antarctic plateau. Therefore, the precipitation frequency and the snowfall rate could be underestimated over this region. On the other hand, because near surface reflectivity is measured about 1300 m over the surface, blowing snow is not confounded with precipitation in peripheral areas, which is usually the main problem for precipitation measurements over this region.

Due to the difficulties for CloudSat to detect precipitation in the interior of the ice sheet, CloudSat precipitation products are more useful in the periphery of the ice sheet than in the interior. However, precipitation in the periphery of the ice sheet is quite important. Three quarters of the total Antarctic precipitation falls in this region, and it is where the models predict the largest precipitation increase over the 21st century (Genthon et al., 2009a).

The lack of ground-based measurements prevents direct validation of CloudSat data. However, agreement between CloudSat data and ERA Interim reanalysis is encouraging for reliability of both datasets. This is consistent with the study of Boening et al. (2012) who have already found good agreement between CloudSat and ERA Interim for the snowfall rate in Antarctica (in the region 30° W–60° E, 65° S–80° S). Even if the spatiotemporal sampling of CloudSat is not really good (between 350 and 500 orbits per grid cell over the Antarctic periphery for the period August 2006–April 2011), the snowfall rate obtained with CloudSat is similar to the snowfall rate predicted by ERA Interim during the same period (Fig. 6). Therefore, the spatiotemporal sampling of CloudSat seems to be sufficient to reproduce statistics of Antarctic precipitation for the period August 2006–April 2011.

CloudSat does not provide any data during the night since April 2011, but the Earth-CARE satellite is scheduled for launch in 2015 into a polar orbit, and will carry a Cloud Profiling Radar (Kumagai et al., 2003). In situ observations are highly desirable to evaluate and improve remote sensing techniques for Antarctic precipitation studies, and could be very useful during the EarthCARE mission. Future spaceborne radar missions should allow us to determine if Antarctic precipitation is increasing due to global warming as predicted by models.

Acknowledgements. This study was supported by the LEFE/CLAPA programme (Institut National des Sciences de l'Univers). This work was partially supported by funding by the ICE2SEA programme from the European Union 7 framework programme, grant number 226 375. Ice2Sea contribution number 176. Funding for this project was provided by a grant from la Région Rhône-Alpes. We are grateful to the Observatoire des Sciences de l'Univers de Grenoble (OSUG) which provided fundings for visits in France and in the USA. Parts of this research by N. B. W. and T. L. were performed at the University of Wisconsin-Madison for the Jet Propulsion Laboratory, California Institute of Technology, sponsored by the National Aeronautics and Space Administration. CloudSat data were obtained from the CloudSat Data Processing Center (http://www.cloudsat.cira.colostate.edu).

References

Arthern, R. J., Winebrenner, D. P., and Vaughan, D. G.: Antarctic snow accumulation mapped using polarization of 4.3 cm wavelength microwave emission, J. Geophys. Res.-Atmos., 111, doi:10.1029/2004JD005667, 2006. 1281, 1288, 1296, 1303

Bamber, J. L., Gomez-Dans, J. L., and Griggs, J. A.: A new 1 km digital elevation model of the Antarctic derived from combined satellite radar and laser data – Part 1: Data and methods, The Cryosphere, 3, 101–111, doi:10.5194/tc-3-101-2009, 2009. 1285, 1299

Barnston, A. G.: Correspondence among the correlation, RMSE, and Heidke forecast verification measures, refinement of the Heidke Score, Weather Forecast., 7, 699–709, 1992. 1287

Bindschadler, R., Choi, H., Shuman, C., and Markus, T.: Detecting and measuring new snow accumulation on ice sheets by satellite remote sensing, Remote Sens. Environ., 98, 388–402, 2005. 1281

Boening, C., Lebsock, M., Landerer, F., and Stephens, G.: Snowfall-driven mass change on the East Antarctic ice sheet, Geophys. Res. Lett., 39, doi:10.1029/2012GL053316, 2012. 1290

Bromwich, D. H.: Snowfall in high southern latitudes, Rev. Geophys., 26, 149–168, 1988. 1281

Bromwich, D. H., Guo, Z., Bai, L., and Chen, Q.-S.: Modeled Antarctic precipitation, Part I: Spatial and temporal variability, J. Climate, 17, 427–447, 2004. 1281

Church, J. A., Clark, P. U., Cazenave, A., Gregory, J. M., Jevrejeva, S., Levermann, A., Merrifield, M. A., Milne, G. A., Nerem, R. S., Nunn, P. D., Payne, A. J., Pfeffer, W. T., Stammer, D., and Unnikrishnan, A. S.: Sea level change, in: Climate Change 2013: The Physical Science Basis, Contribution of Working Group I to the Fifth Assessment Report of the Intergovernmental Panel on Climate Change, edited by: Stocker, T. F., Qin, D., Plattner, G. K., Tignor, M., Allen, S. K., Boschung, J., Nauels, A., Xia, Y., Bex, V., and Midgley, P. M., Cambridge University Press, Cambridge, UK and New York, NY, USA, 2013. 1280

Dee, D. P., Uppala, S. M., Simmons, A. J., Berrisford, P., Poli, P., Kobayashi, S., Andrae, U., Balmaseda, M. A., Balsamo, G., Bauer, P., Bechtold, P., Beljaars, A. C. M., van de Berg, L., Bidlot, J., Bormann, N., Delsol, C., Dragani, R., Fuentes, M., Geer, A. J., Haimberger, L., Healy, S. B., Hersbach, H., Hólm, E. V., Isaksen, L., Kållberg, P., Köhler, M., Matricardi, M., McNally, A. P., Monge-Sanz, B. M., Morcrette, J.-J., Park, B.-K., Peubey, C., de Rosnay, P., Tavolato, C., Thépaut, J.-N., and Vitart, F.: The ERA-Interim reanalysis: configuration and performance of the data assimilation system, Q. J. Roy. Meteor. Soc., 137, 553–597, 2011. 1284, 1286

Eisen, O., Frezzotti, M., Genthon, C., Isaksson, E., Magand, O., van den Broeke, M. R., Dixon, D. A., Ekaykin, A., Holmlund, P., Kameda, T., Karlöf, L., Kaspari, S., Lipenkov, V. Y., Oerter, H., Takahashi, S., and Vaughan, D. G.: Ground-based measurements of spatial and temporal variability of snow accumulation in East Antarctica, Rev. Geophys., 46, doi:10.1029/2006RG000218, 2008. 1280, 1281

Frezzotti, M., Scarchilli, C., Becagli, S., Proposito, M., and Urbini, S.: A synthesis of the Antarctic surface mass balance during the last 800 yr, The Cryosphere, 7, 303–319, doi:10.5194/tc-7-303-2013, 2013. 1280, 1288

Fujita, K. and Abe, O.: Stable isotopes in daily precipitation at Dome Fuji, East Antarctica, Geophys. Res. Lett., 33, doi:10.1029/2006GL026936, 2006. 1281

Genthon, C. and Krinner, G.: Antarctic surface mass balance and systematic biases in general circulation models, J. Geophys. Res.-Atmos., 106, 20653–20664, 2001. 1289

Genthon, C., Krinner, G., and Castebrunet, H.: Antarctic precipitation and climate change predictions: horizontal resolution and margin vs. plateau issues, Ann. Glaciol., 50, 55–60, 2009a. 1280, 1290

Genthon, C., Magand, O., Krinner, G., and Fily, M.: Do climate models underestimate snow accumulation on the Antarctic plateau? A re-evaluation of/from in situ observations in East Wilkes and Victoria Lands, Ann. Glaciol., 50, 61–65, 2009b. 1288

Gregory, J. and Huybrechts, P.: Ice-sheet contributions to future sea-level change, Philos. T. R. Soc. A, 364, 1709–1732, 2006. 1280

Haynes, J. M., L'Ecuyer, T. S., Stephens, G. L., Miller, S. D., Mitrescu, C., Wood, N. B., and Tanelli, S.: Rainfall retrieval over the ocean with spaceborne W-band radar, J. Geophys. Res.-Atmos., 114, doi:10.1029/2008JD009973, 2009. 1282

Hiley, M. J., Kulie, M. S., and Bennartz, R.: Uncertainty analysis for CloudSat snowfall retrievals, J. Appl. Meteorol. Clim., 50, 399–418, 2010. 1281

Kulie, M. S. and Bennartz, R.: Utilizing spaceborne radars to retrieve dry snowfall, J. Appl. Meteorol. Clim., 48, 2564–2580, 2009. 1281

Kumagai, H., Kuroiwa, H., Kobayashi, S., and Orikasa, T.: Cloud profiling radar for EarthCARE mission, P. SPIE Is.&T. Elect. Im., 4894, 118–125, 2003. 1290

Liu, G.: Deriving snow cloud characteristics from CloudSat observations, J. Geophys. Res.-Atmos., 113, doi:10.1029/2007JD009766, 2008. 1281

Monaghan, A. J., Bromwich, D. H., Fogt, R. L., Wang, S.-H., Mayewski, P. A., Dixon, D. A., Ekaykin, A., Frezzotti, M., Goodwin, I., Isaksson, E., Kaspari, S. D., Morgan, V. I., Oerter, H., Van Ommen, T. D., Van der Veen, C. J., and Wen, J.: Insignificant change in Antarctic snowfall since the international geophysical year, Science, 313, 827–831, 2006. 1280, 1288

Rodgers, C.: Inverse Methods for Atmospheric Sounding, vol. 2 of Series on Atmospheric, Oceanic and Planetary Physics, World Scientific, Singapore, 240 pp., 2000. 1282

Simmons, A., Uppala, S., Dee, D., and Kobayashi, S.: ERA-interim: new ECMWF re-analysis products from 1989 onwards, ECMWF Newslett, 110, 25–35, 2006. 1284

Stephens, G. L., Vane, D. G., Tanelli, S., Im, E., Durden, S., Rokey, M., Reinke, D., Partain, P., Mace, G. G., Austin, R., L'Ecuyer, T., Haynes, J., Lebsock, M., Suzuki, K., Waliser, D., Wu, D., Kay, J., Gettelman, A., Wang, Z., and Marchand, R.: CloudSat mission: performance and early science after the first year of operation, J. Geophys. Res.-Atmos., 113, doi:10.1029/2008JD009982, 2008. 1281

Wood, N. B.: Estimation of Snow Microphysical Properties with Application to Millimeter-Wavelength Radar Retrievals for Snowfall Rate, Ph.D. dissertation, Colorado State University, Fort Collins, Colorado, 231 pp., available from http://hdl.handle.net/10217/48170 (last access: February 2014) 2011. 1282

Wood, N. B., L'Ecuyer, T., Vane, D. G., Stephens, G. L., and Partain, P.: Level 2C snow profile process description and interface control document, version 0., Tech. rep., available at: http://www.cloudsat.cira.colostate.edu/ICD/2C-SNOW-PROFILE/2C-SNOW-PROFILE_PDICD_P_R04.pdf (last access: February 2014), 2013. 1282

Title Page
Abstract Introduction
Conclusions References
Tables Figures
◀I ▶I
◀ ▶
Back Close
Full Screen / Esc
Printer-friendly Version
Interactive Discussion

Table 1. Comparison between the precipitation flags from the 2C-PRECIP-COLUMN product and ERA Interim reanalysis at Dumont d'Urville for the period August 2006–April 2011. In ERA Interim reanalysis, precipitation events were defined for a precipitation rate over 0.07 mm 6 h^{-1}. The success rate is the proportion of flags indicating a situation (precipitation/no precipitation) that match with the same situation in ERA Interim. For the precipitation possible, the success rate is the proportion of flags indicating precipitation possible that match with precipitation events in ERA Interim.

Detection	Number of flags	Success rate
Period without precipitation	265	92 %
Precipitation certain	85	91 %
Precipitation possible	38	55 %

Table 2. Comparison between the snowfall rate ($\text{mm}\,\text{yr}^{-1}$) from CloudSat and ERA Interim reanalysis for the period August 2006–April 2011, and the accumulation rate ($\text{mm}\,\text{yr}^{-1}$) from Arthern et al. (2006) for the period 1950–2000. All the rates given in this table are averaged over the surface observed by CloudSat (latitude $< 82^{\circ}$ S).

	Continent	Altitude > 2250 m	Altitude < 2250 m
Snowfall rate from CloudSat	171	36	303
Snowfall rate from ERA Interim	163	49	273
Accumulation rate from Arthern et al.	163	81	243

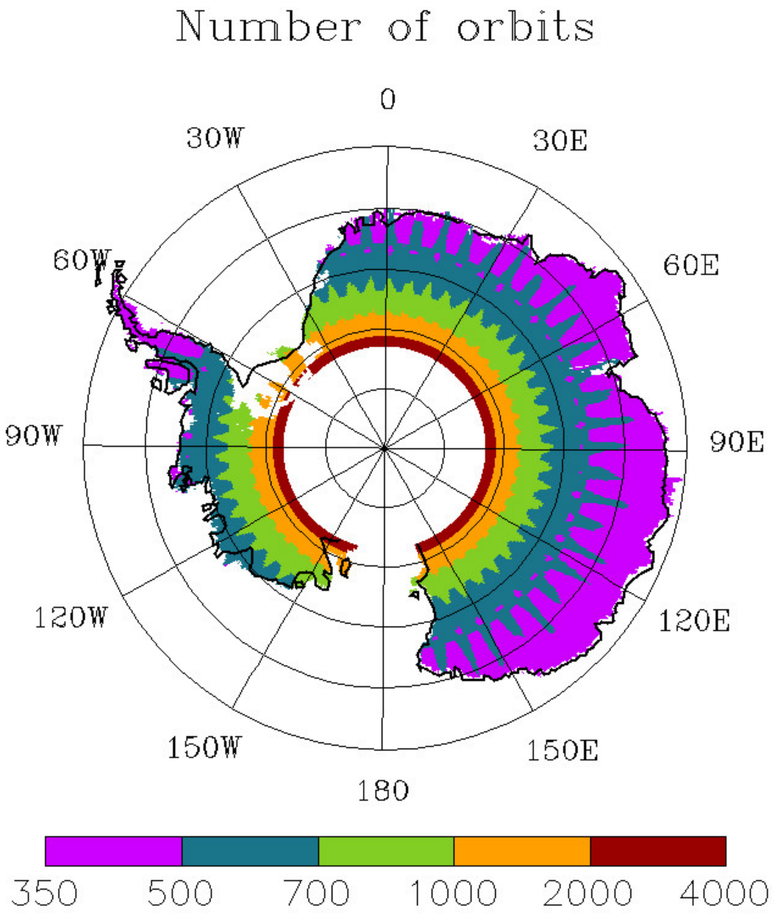

Fig. 1. Total number of orbits per grid cell from August 2006 to April 2011.

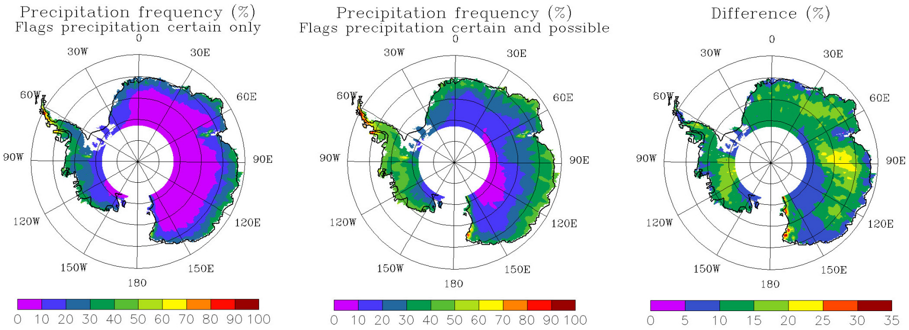

Fig. 2. Precipitation frequency (%) with the flags sorted as precipitation certain (left), and with the flags sorted as precipitation certain and possible (middle) for the period August 2006–April 2011. The difference between the two maps (right).

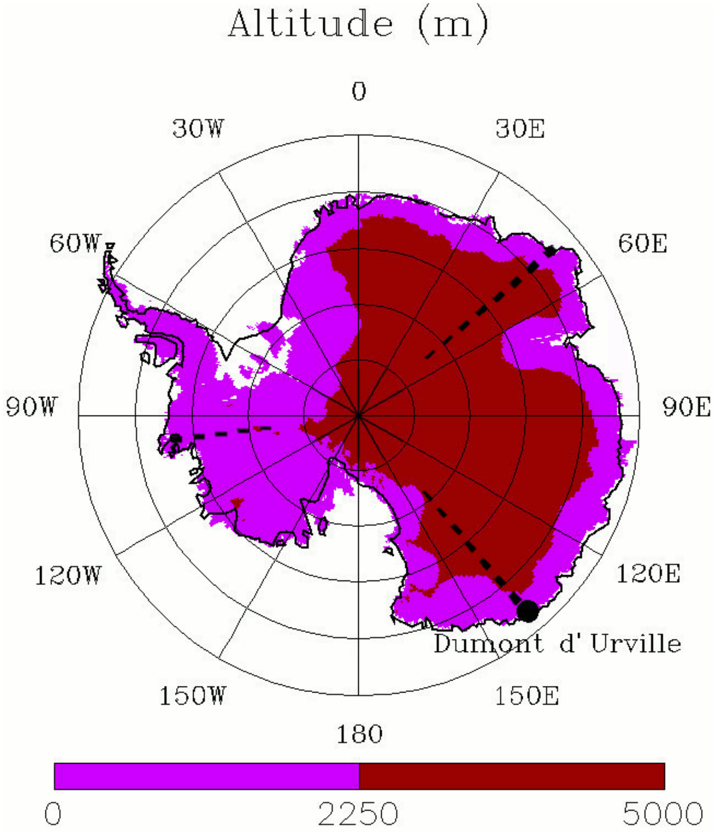

Fig. 3. The 2250 m elevation contour derived from the digital elevation model of Bamber et al., 2009. The part of the ice sheet with surface elevation over 2250 m (red), and below 2250 m (purple). The black dot indicates the location of Dumont d'Urville station. The transects from Fig. 5 are also shown on the map.

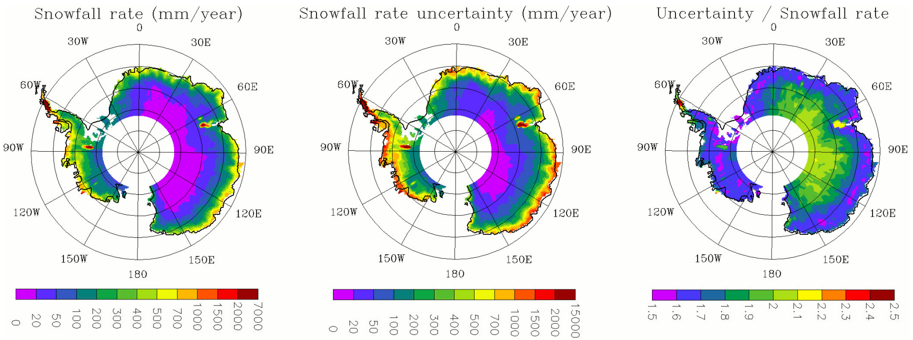

Fig. 4. Mean annual snowfall rate (mm water equivalent/year) from the 2C-SNOW-PROFILE product (left) and mean single retrieval uncertainty (middle) for the period August 2006–April 2011. The ratio of the uncertainty over the snowfall rate (right).

Title Page
Abstract
Introduction
Conclusions
References
Tables
Figures
◀I
▶I
◀
▶
Back
Close
Full Screen / Esc
Printer-friendly Version
Interactive Discussion

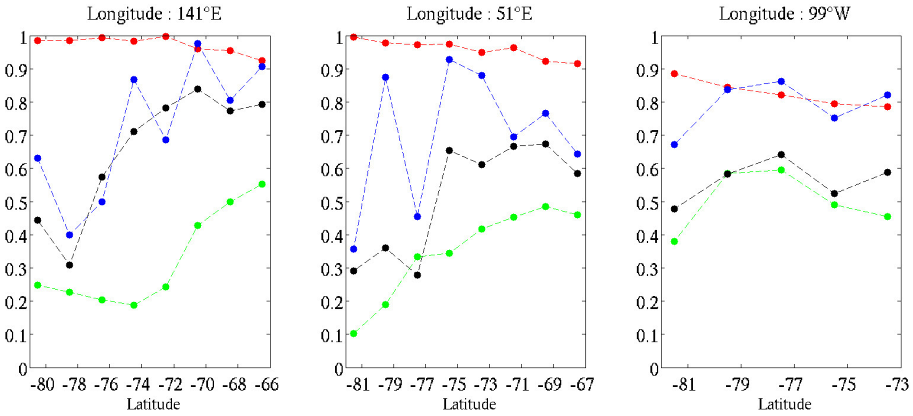

Fig. 5. Comparison between the precipitation flags from the 2C-PRECIP-COLUMN product and ERA Interim reanalysis for the period August 2006–April 2011. In ERA Interim reanalysis, precipitation events were defined for a precipitation rate over 0.07 mm 6 h^{-1}. Red curve: proportion of flags indicating periods without precipitation that match with periods without precipitation in ERA Interim. Blue curve: proportion of flags indicating precipitation certain that match with precipition events in ERA Interim. Green curve: proportion of flags indicating precipitation possible that match with precipitation events in ERA Interim. Black curve: Heidke Skill Score assessed using flags sorted as precipitation certain and period without precipitation.

Title Page
Abstract
Introduction
Conclusions
References
Tables
Figures
◀|
|▶
◀
▶
Back
Close
Full Screen / Esc
Printer-friendly Version
Interactive Discussion

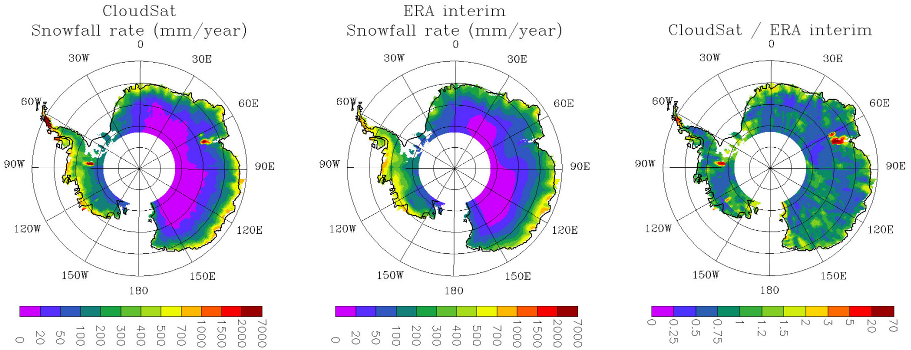
CloudSat
Snowfall rate (mm/year)

ERA interim
Snowfall rate (mm/year)

CloudSat / ERA interim

Fig. 6. Mean annual snowfall rate (mm water equivalent/year) from CloudSat (left) and ERA Interim reanalysis (middle) from August 2006 to April 2011. The ratio of the snowfall rate from CloudSat over the snowfall rate from ERA Interim (right).

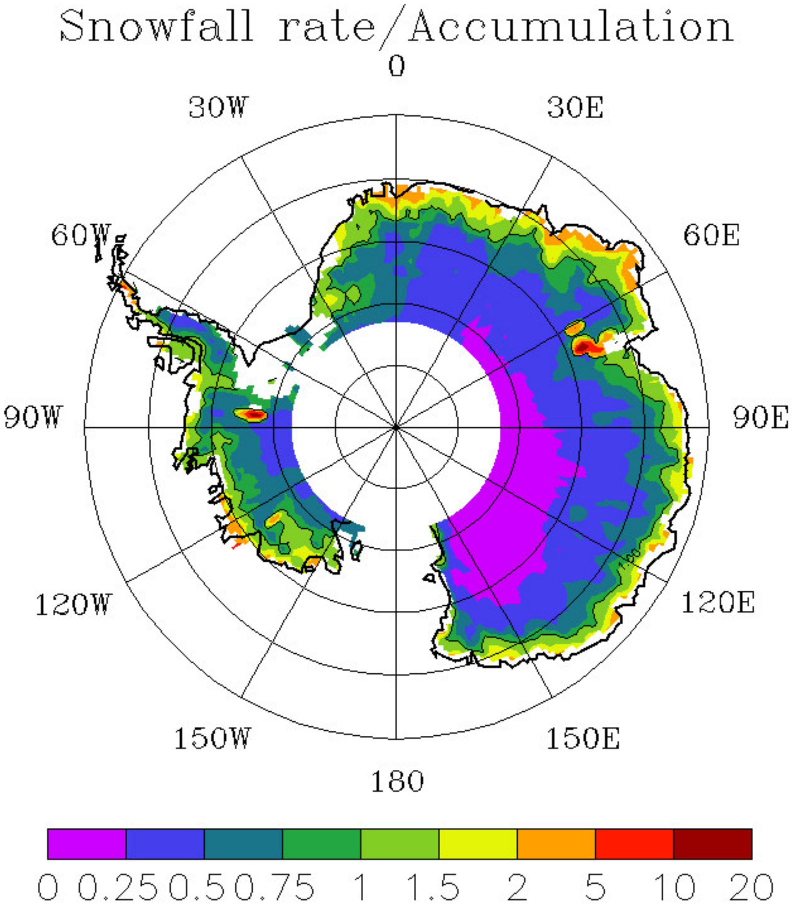

Fig. 7. Ratio of the snowfall rate observed by CloudSat for the period August 2006–April 2011 over the accumulation rate determined by Arthern et al. (2006) for the period 1950–2000. The isoline 1 is shown on the map.

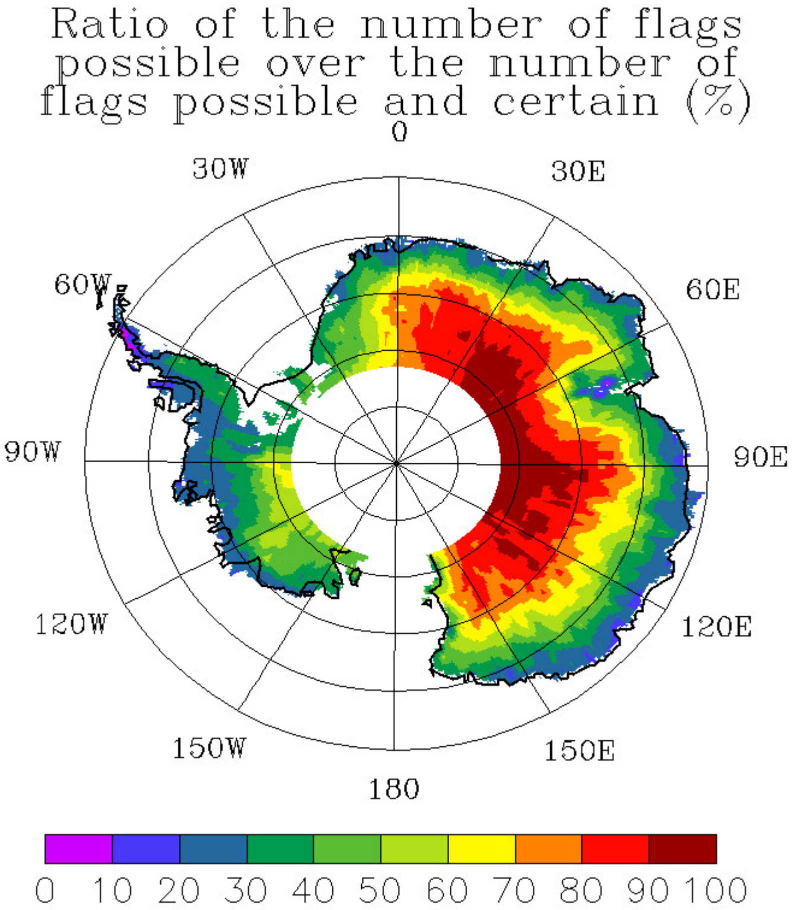

Fig. 8. Ratio of the number of flags indicating precipitation possible over the number of flags indicating precipitation possible and certain (%).